Mifsud, Duncan V., Herczku, Péter, Ramachandran, Ragav, Sundararajan, Pavithraa, Rahul, K K, Kovács, Sándor T S, Sulik, Béla, Juhász, Zoltán, Rácz, Richárd, Biri, Sándor and others (2024) *A systematic mid-infrared spectroscopic study of thermally processed H2S ices.* Spectrochimica acta. Part A, Molecular and biomolecular spectroscopy, 319 . ISSN 1386-1425.

A systematic mid-infrared spectroscopic study of thermally processed H2S ices

Duncan V. Mifsud [a,b], Péter Herczku [b], Ragav Ramachandran [c], Pavithraa Sundararajan [c], K.K. Rahul [b], Sándor T.S. Kovács [b], Béla Sulik [b], Zoltán Juhász [b], Richárd Rácz [b], Sándor Biri [b], Zuzana Kaňuchová [d], Sergio Ioppolo [e], Bhalamurugan Sivaraman [c], Robert W. McCullough [f], Nigel J. Mason [a,b,*]

[a] *Centre for Astrophysics and Planetary Science, School of Physics and Astronomy, University of Kent, Canterbury CT2 7NH, United Kingdom*
[b] *HUN-REN Institute for Nuclear Research (Atomki), Debrecen H-4026, Hungary*
[c] *Atomic, Molecular, and Optical Physics Division, Physical Research Laboratory, Ahmedabad 380009, India*
[d] *Astronomical Institute, Slovak Academy of Sciences, Tatranská Lomnica SK-059 60, Slovakia*
[e] *Centre for Interstellar Catalysis, Department of Physics and Astronomy, Aarhus University, Aarhus DK-8000, Denmark*
[f] *Department of Physics and Astronomy, School of Mathematics and Physics, Queen's University Belfast, Belfast BT7 1NN, United Kingdom*

HIGHLIGHTS

- H2S ices were deposited at 20, 40, and 70 K and warmed to sublimation.
- Changes in the acquired mid-infrared spectra were quantitatively studied.
- A phase change from an amorphous to a crystalline structure was observed by 60 K.
- Extensive absorption band splitting was observed as a result of crystallisation.
- Our results may prove useful to the detection of H2S in astronomical environments.

GRAPHICAL ABSTRACT
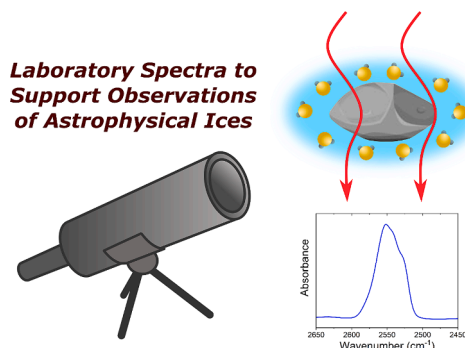
ARTICLE INFO

ABSTRACT

The positive identification of the molecular components of interstellar icy grain mantles is critically reliant upon the availability of laboratory-generated mid-infrared absorption spectra which can be compared against data acquired by ground- and space-borne telescopes. However, one molecule which remains thus far undetected in interstellar ices is H2S, despite its important roles in astrochemical and geophysical processes. Such a lack of a detection is surprising, particularly in light of its relative abundance in cometary ices which are believed to be the most pristine remnants of pre-solar interstellar ices available for study. In this paper, we present the results of an extensive and quantitative mid-infrared spectroscopic characterisation of H2S ices deposited at 20, 40, and 70 K and thermally processed to sublimation in an ultrahigh-vacuum system. We anticipate our results to be useful

in confirming the detection of interstellar H_2S ice using high-resolution and high-sensitivity instruments such as the *James Webb Space Telescope*, as well as in the identification of solid H_2S in icy environments in the outer Solar System, such as comets and moons.

1. Introduction

Spectroscopy has played a key role in unravelling the molecular composition of the cosmos. Indeed, the majority of the 300 or so molecules known to be present in interstellar and circumstellar media were first identified through their rotational emission spectra [1]. However, although the utility of rotational spectroscopy in identifying the gas-phase molecular components of interstellar space is perhaps unparalleled [2,3], the restriction of rotational motion in solids means that alternative spectroscopic techniques are required to characterise the chemical compositions of ices adsorbed to the nanoscale dust grains embedded within dense molecular clouds. Infrared absorption spectroscopy thus represents a preferred technique in this regard, and young stellar objects located within or behind dense molecular clouds (from the perspective of the Earth) are used as infrared radiation sources. As this radiation traverses the cloud it is absorbed by solid-phase molecules at frequencies characteristic to their vibrational quantum levels and the transmitted radiation may then be measured by a ground- or space-borne telescope thus allowing for an infrared absorption spectrum to be produced [4].

The interpretation of the infrared spectra of observed interstellar objects and the identification of molecules present in interstellar ices requires the availability of laboratory data generated under simulated interstellar conditions for comparative purposes. To this end, multiple research groups in the field of laboratory astrochemistry have dedicated significant effort to the spectroscopic characterisation of interstellar ice analogues under various experimental conditions, and a number of databases have been established [5,6]. Our laboratory has also contributed to the mid-infrared spectroscopic characterisation of low-temperature molecular solids relevant to astrochemistry, with systematic studies on CO_2, O_3, and SO_2 having been published in recent years [7–9]. In this present paper, we extend our previous studies by considering the mid-infrared absorption spectroscopy of H_2S interstellar ice analogues deposited at three different temperatures and thermally processed to sublimation.

The identification of solid H_2S in interstellar icy grain mantles has proven to be challenging [10]. Indeed, recent observational data of the Chamaeleon I dense cloud acquired by the *James Webb Space Telescope* along the line of sight towards the background star NIR38 has only allowed for an upper limit of 0.64 % (relative to the cloud's H_2O ice content) to be calculated [11], while other sulphurous molecules such as OCS and SO_2 have been detected with significantly greater certainty in the dense interstellar medium [4,11]. These observational data contrast with the fact that H_2S is known to be the most abundant sulphurous molecule in a number of cometary nuclei [12–14] and, therefore, should also be an important reservoir of molecular sulphur in the dense interstellar medium. If this is true, then it is possible to envisage a H_2S formation mechanism involving the hydrogenation of sulphur atoms adsorbed on the surface of an interstellar dust grain, based on the typical known efficiency of surface-catalysed hydrogenation reactions under interstellar conditions [15]. Indeed, analogous reactions involving oxygen atoms, carbon atoms, nitrogen atoms, and CO molecules are known to respectively contribute to the presence of H_2O, CH_4, NH_3, and CH_3OH in interstellar icy grain mantles [16–19]. It is interesting to note, however, that although the surface-catalysed hydrogenation of sulphur atoms has not, to the best of our knowledge, been studied experimentally, density functional theory calculations have suggested that this synthesis route is associated with high activation energy barriers [20,21].

Nevertheless, the presence and relative abundance of H_2S in cometary nuclei is suggestive of the existence of some physical or chemical process by which it accumulates during the early stages of the evolution of interstellar space. This therefore provides a strong motivation for acquiring laboratory-generated mid-infrared absorption spectra of solid H_2S at various temperatures and under different deposition conditions which may then be used in combination with observational data acquired by telescopes to determine if H_2S ice is present in different interstellar media (e.g., dense clouds, hot cores and corinos, proto-stellar and proto-planetary discs). Indeed, a number of studies on the infrared spectroscopy of solid H_2S have been performed over the past seven decades [22–29], with the most detailed arguably being that of Fathe et al. [27] who reported the spectra of H_2S and its isotopologue D_2S at temperatures of 10 and 70 K. In their study, Fathe et al. [27] found that the most prominent mid-infrared absorption bands of solid, low-temperature H_2S are attributable to the stretching modes (ν_s) located at about 2550 cm^{-1} and the bending mode (ν_2) located at about 1170 cm^{-1}, whose positions have been consistently confirmed by previous and subsequent studies (Table 1).

It is interesting to note that, under cryogenic and ambient pressure conditions, solid H_2S presents a particularly interesting phase chemistry, with no fewer than three crystalline phases known to exist. These phases are designated using numbers and are accordingly termed phases I, II, and III and are characterised by ambient pressure transition temperatures of 126.2 (I → II) and 103.5 K (II → III) [27]. The higher temperature phases I and II are orientationally disordered, meaning that they are ordered with respect to the sulphur atoms but not with respect to the hydrogen atoms, and thus exhibit very broad bands corresponding to the ν_s modes which are only slightly narrower than the analogous band of the amorphous ice. This contrasts greatly with the ordered phase III, which exhibits a significantly narrower band attributable to the ν_s mode in which individual stretching modes emerge as distinct sub-structures. Moreover, bands associated with both the symmetric stretching mode (ν_1) and the ν_2 mode undergo splitting in the phase III ice due to the existence of two unique sulphur atoms but three unique S–H bonds in the eight-molecule unit cell [30–32]. However, under conditions relevant to astrochemistry (i.e., cryogenic temperatures and high- to ultrahigh-vacuum pressures), the only crystalline phase of importance is phase III (hereafter referred to simply as the H_2S crystalline phase).

In this present paper, we have explored in detail the mid-infrared absorption spectroscopy of pure H_2S ices prepared at temperatures of 20, 40, and 70 K under ultrahigh-vacuum conditions and subsequently thermally processed to sublimation, with a particular focus on the ν_s and ν_2 modes. By making use of a systematic methodology to investigate the spectroscopic response of H_2S to thermal processing and its variation among ices prepared at different temperatures, our results extend those of previous works and are also likely to be of use in identifying the presence and structure of H_2S ice in extra-terrestrial environments (such as the interstellar medium) by high-resolution and high-sensitivity instruments such as the *James Webb Space Telescope*.

2. Experimental methodology

All experimental work was carried out using the Ice Chamber for Astrophysics-Astrochemistry (ICA); a set-up for laboratory astrochemistry located at the HUN-REN Institute for Nuclear Research (Atomki) in Debrecen, Hungary. The set-up has been described in some detail in previous publications [33,34], and so only an overview of its most salient features will be provided in this paper. The ICA is an ultrahigh-vacuum chamber with an operational base pressure of a few 10^{-9} mbar which is maintained by the combined action of a turbomolecular

pump and a scroll pump. Within the centre of the chamber is a gold-coated oxygen-free high-conductivity copper sample holder into which four infrared-transparent substrates (in this case, ZnSe) may be mounted. The sample holder is maintained in contact with the cold finger of a closed-cycle helium cryostat which allows it to be cooled to 20 K. Temperature regulation in the range 20–300 K is achieved by setting an equilibrium between an internal cartridge heater and the cooling effect of the cryostat.

Pure H_2S ices were prepared on the cooled ZnSe deposition substrates via the background deposition of H_2S gas (99.5 % purity, supplied by Linde). The gas was first introduced into a pre-mixing line before being dosed into the main chamber at a pressure of a few 10^{-6} mbar, which corresponds to an average ice thickness growth rate of about 0.04 μm min^{-1}. The growth and subsequent thermal processing of the ices were monitored in situ by Fourier-transform mid-infrared transmission absorption spectroscopy (spectral range = 4000–650 cm^{-1}; spectral resolution = 0.5 cm^{-1}; 256 scans per spectrum) using a Thermo Nicolet Nexus 670 spectrophotometer and by maintaining the infrared spectroscopic beam at normal incidence to the ice samples. Pure H_2S ices were deposited at temperatures of 20, 40, and 70 K and then warmed at a rate of 2 K min^{-1}, with mid-infrared spectra being acquired at successive 10 K intervals until complete sublimation of the ice was recorded. Prior to the acquisition of a spectrum at a given temperature, the ice was allowed up to five minutes to equilibrate, during which time no isothermal changes in the appearance of any of the spectra were observed. A summary of the experiments performed in this study is provided in Table 2.

The amount of ice deposited in a given experiment is assessed quantitatively using mid-infrared spectra collected after deposition of the ice but prior to any thermal processing. The molecular column density N (molecules cm^{-2}) of a deposited ice is related to the integrated absorbance S (cm^{-1}) of one of its characteristic absorption bands as follows:

$$N = \ln(10)\frac{S}{A} \tag{1}$$

where A is the integrated strength constant (cm molecule^{-1}) for that particular band (which, in this study, we have taken to be 1.69×10^{-17} cm molecule^{-1} for the ν_s mode) [29]. The constant $\ln(10)$ is included in the equation so as to relate S, which is measured on an absorbance scale,

Table 2

Summary of the thermal annealing experiments performed in this study. Column densities, N, and ice thicknesses, h, were calculated by integrating the absorbance of the ν_s modes between 2600–2500 cm^{-1}.

H_2S Ice	Deposition T (K)	N (10^{18} molecules cm^{-2})	h (μm)
1	20	1.47 ± 0.10	0.882 ± 0.063
2	40	0.93 ± 0.07	0.422 ± 0.030
3	70	1.17 ± 0.08	0.530 ± 0.038

Table 1

Review of the major mid-infrared absorption features of H_2S ice (and some isotopologues). Band peak positions for an amorphous ice (prepared at 20 K) and a crystalline ice (prepared at 100 K) investigated in this study are included for comparative purposes.

Mode	Assignment	Band Position (cm^{-1})									
		Reference A	Reference B	Reference C	Reference D	Reference E	Reference F	Reference G	Reference H	This Study Amorphous	Crystalline
ν_s	$H_2^{32}S$	2548	–	–	–	–	–	–	2548	2551.0	–
	$D_2^{32}S$	1853	–	–	–	–	–	–	–	–	–
ν_1	$H_2^{32}S$ (A$_{2u}$)	–	2525	2523	2523	2523	2526	2523.7	–	–	2524.6
	$H_2^{32}S$ (E$_u$)	–	2536	2532	2532	2532	2535	2533.5	–	–	2535.8
	$D_2^{32}S$ (A$_{2u}$)	–	1832	1835	1835	–	–	1832.0	–	–	–
	$D_2^{32}S$ (E$_u$)	–	1840	1843	1843	–	–	1840.0	–	–	–
ν_2	$H_2^{32}S$	1168	–	–	–	–	–	–	1168	–	–
	$H_2^{32}S$ (A$_{2u}$)	–	1169	1171	1171	1171	1169	1170.0	–	–	1168.9
	$H_2^{32}S$ (E$_u$)	–	1184	1186	1186	1186	1184	1185.0	–	–	1183.9
	HD^{32}S	–	–	1026	–	–	–	1028.0	–	–	–
	$D_2^{32}S$	846	860	–	–	–	–	–	–	–	–
	$D_2^{32}S$ (A$_{2u}$)	–	846	847	847	–	–	846.0	–	–	–
	$D_2^{32}S$ (E$_u$)	–	856	857	857	–	–	856.5	–	–	–
ν_3	$H_2^{32}S$	–	2548	2544	2544	2544	2547	2545.0	–	–	2545.7
	$D_2^{32}S$	–	1852	1854	1854	–	–	1854.0	–	–	–
$\nu_s + \nu_2$	$H_2^{32}S$	3704	–	–	–	–	–	–	–	3711.5	–
	$D_2^{32}S$	2693	–	–	–	–	–	–	–	–	–
$\nu_s + \nu_R$	$H_2^{32}S$	2715	–	–	–	–	–	–	–	–	–
$\nu_s + \nu_T$	$H_2^{32}S$	2642	–	–	–	–	–	–	–	2635.7	–
	$D_2^{32}S$	1942	–	–	–	–	–	–	–	–	–
$\nu_1 + \nu_2$	$H_2^{32}S$	–	3682	–	–	–	3683	–	–	–	3694.3
	$D_2^{32}S$	–	2671	–	–	–	–	–	–	–	–
$\nu_2 + \nu_3$	$H_2^{32}S$	–	3694	–	–	–	3695	–	–	–	–
	$D_2^{32}S$	–	2687	–	–	–	–	–	–	–	–
$\nu_3 + \nu_R$	$H_2^{32}S$	–	2722	–	–	–	2720	–	–	–	–
$\nu_3 + \nu_T$	$H_2^{32}S$	–	2636	–	–	–	2635	–	–	–	2628.1
	$D_2^{32}S$	–	1938	–	–	–	–	–	–	–	–

Reference A: Fathe et al. [27] for an amorphous ice at 10 K; Reference B: Fathe et al. [27] for a crystalline ice at 70 K; Reference C: Reding and Hornig [22] for a crystalline ice at 63 K; Reference D: Miller and Leroi [23] for a crystalline ice at 80 K; Reference E: Ferraro and Fink [25] for a crystalline ice at 62 K; Reference F: Ferraro et al. [26] for a crystalline ice at 89 K; Reference G: Anderson et al. [24] for a crystalline ice at 18 K; Reference H: Hudson and Gerakines [28] for an amorphous ice at 16 K.

to N, which is measured on an optical depth scale. The thickness h (μm) of the deposited ice may then be calculated as:

$$h = 10^4 \frac{Nm}{\rho N_a} \tag{2}$$

where m is the molar mass of the H_2S ice (34 g mol^{-1}), ρ is its density (amorphous = 0.944 g cm^{-3}; crystalline = 1.244 g cm^{-3}) [29,35], and N_a is the Avogadro constant (6.02 × 10^{23} molecules mol^{-1}). The constant value 10^4 is included to express h in units of μm.

It should be noted that the value for A that was used was calculated for an amorphous H_2S ice prepared at 10 K [29], while the ρ values for amorphous and crystalline H_2S were measured for ices deposited at 19 and 80 K, respectively [29,35]. However, it is very likely that the actual values of A and ρ vary as a function of temperature. Indeed, such variations have been systematically measured for other ices (e.g., CO and CH_3OH) over defined temperature ranges [36,37]. To the best of our knowledge, however, no previous study has undertaken the systematic measurement of the A and ρ values of H_2S at different temperatures. Therefore, the magnitude of the uncertainty introduced into our column density and ice thickness measurements as a result of using A and ρ values defined for H_2S ices deposited at temperatures that differ to those studied herein is unclear; although it should be noted that this does not affect the spectroscopic characterisation of the most prominent H_2S absorption bands discussed in this paper. However, if it is assumed that the temperature dependences of the A and ρ values used herein are not a source of uncertainty in our experiments, then it is possible to calculate the uncertainty in our column density and ice thickness measurements through standard propagation-of-error calculations using an estimated 5 % measurement error in the value of S and published uncertainty values for A and ρ [29,35] (Table 2).

3. Spectroscopic results and discussion

Mid-infrared absorption spectra of amorphous and crystalline H_2S ices (exemplified by the ices respectively deposited at 20 and 70 K) are shown in Fig. 1. The only absorption feature that is evident in the spectrum of the amorphous ice is the broad band corresponding to the ν_s mode at 2551.0 cm^{-1}. In the spectrum of the crystalline ice, this broad band is better resolved into its individual ν_1 and antisymmetric stretching (ν_3) modes, the former of which undergoes splitting due to the

non-equivalence of the number of sulphur atoms and S–H bonds in the unit cell, as discussed previously [30–32]. Interestingly, a band related to the ν_2 mode (which also undergoes splitting for similar reasons as the ν_1 mode) is only observable in the spectrum of the crystalline ice. Although it is likely that the ν_s mode bands will be of significantly greater use in the detection of H_2S ice in extra-terrestrial environments such as the interstellar medium or the outer Solar System, a detailed mid-infrared spectroscopic characterisation of both the ν_s and the ν_2 modes will be provided in the remainder of this section.

3.1. The stretching modes

The thermal evolution of the bands ascribed to the ν_s modes in the spectra of the H_2S ices deposited at 20, 40, and 70 K is depicted in Fig. 2. In the first instance, it is possible to note that the initial appearance of the ν_s mode band for the ice deposited at 20 K differs significantly compared to those of the ices deposited at higher temperatures. In the case of the former, this band takes on a broad, irregularly-shaped profile peaking at 2551.0 cm^{-1} while, in the case of the latter, contributions from the individual sub-components of this vibrational mode (from highest to lowest wavenumber position, the ν_3, ν_1 (E$_u$), and ν_1 (A$_{2u}$) bands) are immediately obvious. Such an observation is indicative of the greater degrees of structural order (i.e., crystallinity) of the ices deposited at higher temperatures.

The thermal processing of the ice deposited at 20 K results in a number of changes in the profile, peak position, integrated absorbance, and peak height of the broad ν_s mode band (Fig. 3). Upon reaching 30 K, the band peak blue-shifts slightly to 2552.3 cm^{-1} and a second peak at 2527.3 cm^{-1} becomes visible. These peaks respectively correspond to the ν_3 and ν_1 (A$_{2u}$) modes, and their emergence against the broad absorption feature indicates the onset of a phase transition from an amorphous structure to a more ordered phase. As the temperature of the ice is further raised, both these peaks red-shift by up to 3.5 cm^{-1} until 50 K, at which point a third peak attributable to the ν_1 (E$_u$) mode becomes evident at 2535.6 cm^{-1}. Warming to higher temperatures results in somewhat distinct responses from these three bands. For instance, the ν_1 (A$_{2u}$) mode red-shifts by 2.4 cm^{-1} across the 50–80 K temperature range, while the ν_1 (E$_u$) mode does not vary as significantly (within 1.2 cm^{-1}) across this temperature range. The ν_3 mode, on the other hand, red-shifts by 1.7 cm^{-1} to 2547.3 cm^{-1} at 60 K, and thereafter incrementally blue-shifts by 0.8 cm^{-1} by the point 80 K is reached.

The emergence of the individual sub-components of the ν_s mode as a result of the thermally induced structural reorganisation of the H_2S ice to a more crystalline phase has a marked effect on the overall integrated absorbance (measured over a wavenumber range of 2600–2500 cm^{-1} using a linear baseline) and the maximum peak height H (dimensionless) of the band. This latter parameter corresponds to the maximum absorbance of the band, and is associated with the broad ν_s mode band in the case of amorphous ices and the emergent ν_3 mode band in the case of ices exhibiting greater degrees of structural order. As can be seen in Fig. 3, on warming the H_2S ice deposited at 20 K to 70 K the integrated absorbance of the ν_s mode band increases by more than 30 % of its original value, while the maximum peak height more than triples with respect to its original value. Slight decreases in both these parameters are noted on further warming of the ice to 80 K, likely due to some mass loss due to sublimation. Indeed, by 90 K, the entire ice had completely sublimed from the deposition substrate.

A closer inspection of the irregular profile of the broad band attributed to the ν_s modes for the ice at 20 K reveals that it is likely to be composed of different contributing absorptions (Fig. 1). Such an observation suggests that it is likely that the H_2S ice did not adopt a purely amorphous structure when deposited at 20 K, but rather was some admixture of amorphous and crystalline in which the amorphous component was dominant. Indeed, the difficulties in preparing purely amorphous ice structures at low temperatures have been reported for a number of simple molecules, including CH_4, CO_2, and N_2O [38–40], and
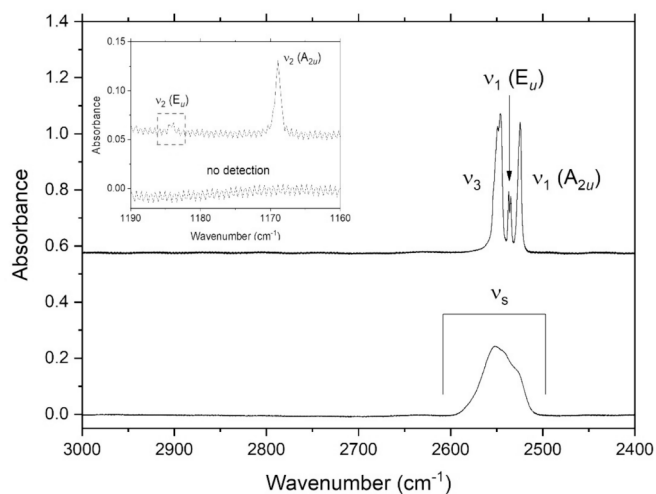
Fig. 1. Mid-infrared absorption spectra of amorphous (lower plot) and crystalline (upper plot) H_2S ices deposited at temperatures of 20 and 70 K, respectively. The estimated thicknesses of the amorphous and crystalline ices are 0.882 ± 0.063 and 0.530 ± 0.038 μm, respectively. Note that spectra are vertically offset for clarity. The inset depicts the weak band corresponding to the ν_2 mode which is not visible in the spectrum of the amorphous ice.
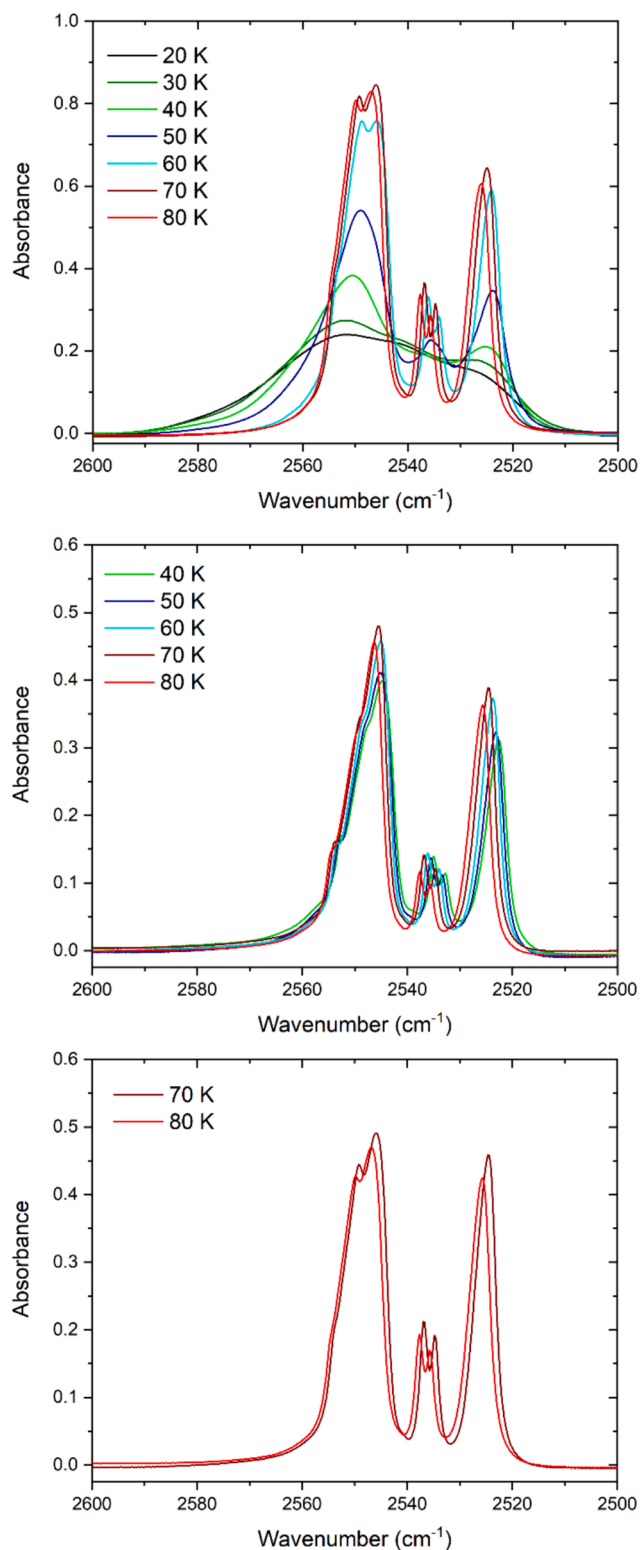
Fig. 2. Thermal evolution of the band attributed to the H$_2$S ν_s modes for ices deposited at 20, 40, and 70 K. Note the readily observable presence of the individual ν_3, ν_1 (E$_u$), and ν_1 (A$_{2u}$) modes (in order from highest to lowest wavenumber position) in the crystalline ices.

Fig. 3. Variations in the integrated absorbance S (top panel), peak height H (middle panel) and peak positions ν (bottom panel) of the ν_s modes for H$_2$S ices deposited at 20 (black circles), 40 (red circles), and 70 K (blue circles). Note that the variations in S and H are reported relative to their initial values S_0 and H_0 upon deposition of the ice. Error bars have been omitted for clarity, but upper bounds to the uncertainties associated with S / S_0, H / H_0, and ν have been calculated to be $\pm$ 7 %, $\pm$15 %, and $\pm$ 0.25 cm^{-1}, respectively.

thus similar difficulties may exist in preparing purely amorphous H$_2$S ice. Nevertheless, the broadness of this absorption feature and the lack of any distinct band sub-components allows us to propose that, to a first approximation, the H$_2$S ice deposited at 20 K is largely amorphous.

Our spectroscopic analyses summarised in Figs. 2 and 3 allow us to

propose that the thermally induced crystallisation of an amorphous H$_2$S ice deposited at 20 K occurs gradually but is largely complete by 60 K. Indeed, even upon initial warming to 30 K, the first tell-tale signs of structural reorganisation within the ice become apparent in the form of the emergent band ascribed to the ν_1 (A$_{2u}$) mode. Further warming increases the extent of crystallisation, but it is not until 50 K that band corresponding to the ν_1 (E$_u$) mode is truly evident. However, at this

temperature, the profiles of these bands are still fairly broad and it is not until 60 K that they adopt a narrower profile akin to those of the crystalline ice shown in Fig. 1.

It is, however, interesting to note that stark differences exist in the appearance of the bands attributed to the ν_s modes of H_2S in an ice that is deposited at 40 K compared to one deposited at 20 K and subsequently thermally processed to 40 K (Figs. 2 and 3). In the case of the latter, these bands are still fairly broad and the ν_1 (E_u) mode has yet to emerge against the background, which is indicative of an ice that still has a significant amorphous component. However, in the case of the former, all of the ν_3, ν_1 (E_u), and ν_1 (A_{2u}) bands are readily apparent and, indeed, the overall spectroscopic profile of the ν_s modes is suggestive of a structurally ordered ice with a dominant crystalline component, with relatively narrow and intense bands. Moreover, thermal processing of the ice deposited at 40 K does not result in any significant variation in the integrated absorbance S of the ν_s mode band, nor in the maximum peak height H (Fig. 3). Such observations contrast with the H_2S ice deposited at 20 K which, even after being warmed to 40 K, continues to experience large increases in both its integrated absorbance and its maximum peak height as it is warmed to even higher temperatures. This is evidence of the fact that an ice deposited at a given temperature will be more structurally ordered (i.e., crystalline) compared to an ice deposited at a lower temperature and subsequently warmed to that given temperature; and echoes the results of our previous study on SO_2 [9]. It is to be noted that the H_2S ice deposited at 70 K is wholly crystalline, with the ν_s mode exhibiting bands with the expected profile of a crystalline ice [27,28], and very little variation in the integrated absorbance or maximum peak height induced by thermal processing being recorded, except for a moderate decrease in the former on going from 70 to 80 K due to sublimation-induced losses of the ice.

3.2. The bending mode

The thermal evolution of the band attributed to the ν_2 mode of solid H_2S is shown in Fig. 4. As can be seen, no detection of this band was made upon preparation of the H_2S ice at 20 K, nor upon its thermal processing to 30 K. However, at 40 K, a weak and broad absorption feature attributable to the ν_2 (A_{2u}) mode band begins to emerge against the background continuum at 1169.0 cm^{-1}. By 50 K, this band is clearly identifiable and at 60 K a second band attributable to the ν_2 (E_u) mode emerges at 1184.1 cm^{-1}. These bands continue to increase in intensity as the temperature of the ice is raised further and remain visible in the spectrum until sublimation occurs by 90 K. Such findings complement well the previous observations made on the thermal evolution of the ν_s mode and suggest that a significant thermally induced restructuring of the ice begins to occur at about 40 K, although at this temperature the ice is still likely characterised by a significant amorphous component as evidenced by the lack of a visible ν_2 (E_u) mode band in Fig. 4. It is evident that, at 50 K, the ice has adopted a significantly more ordered structure and, by a temperature of 60 K, the ice is likely to be largely crystalline as indicated by the appearance of all the split bands of the ν_1 and ν_2 vibrational modes.

Interestingly, when deposited at 40 K, the spectrum of the H_2S ice clearly exhibits bands for both the ν_2 (A_{2u}) and the ν_2 (E_u) modes (Fig. 4), thus contrasting strongly with the appearance of the spectrum for the ice deposited at 20 K and subsequently warmed to 40 K. When deposited at 40 K, it is apparent that solid H_2S is already structurally ordered and contains a significant crystalline component, as evidenced by the fact that not only are both the ν_2 (A_{2u}) and the ν_2 (E_u) bands easily identifiable (Fig. 4), but also by the fact that the ν_1 mode is already split into its own A_{2u} and E_u bands (Fig. 2). Once again, these spectroscopic observations are evidence of the greater degree of structural order (i.e., crystallinity) in a molecular ice deposited at a given temperature compared to one deposited at a lower temperature and subsequently thermally processed to that given temperature. With regards to the H_2S ice deposited at 70 K, the mid-infrared absorption spectrum displays the
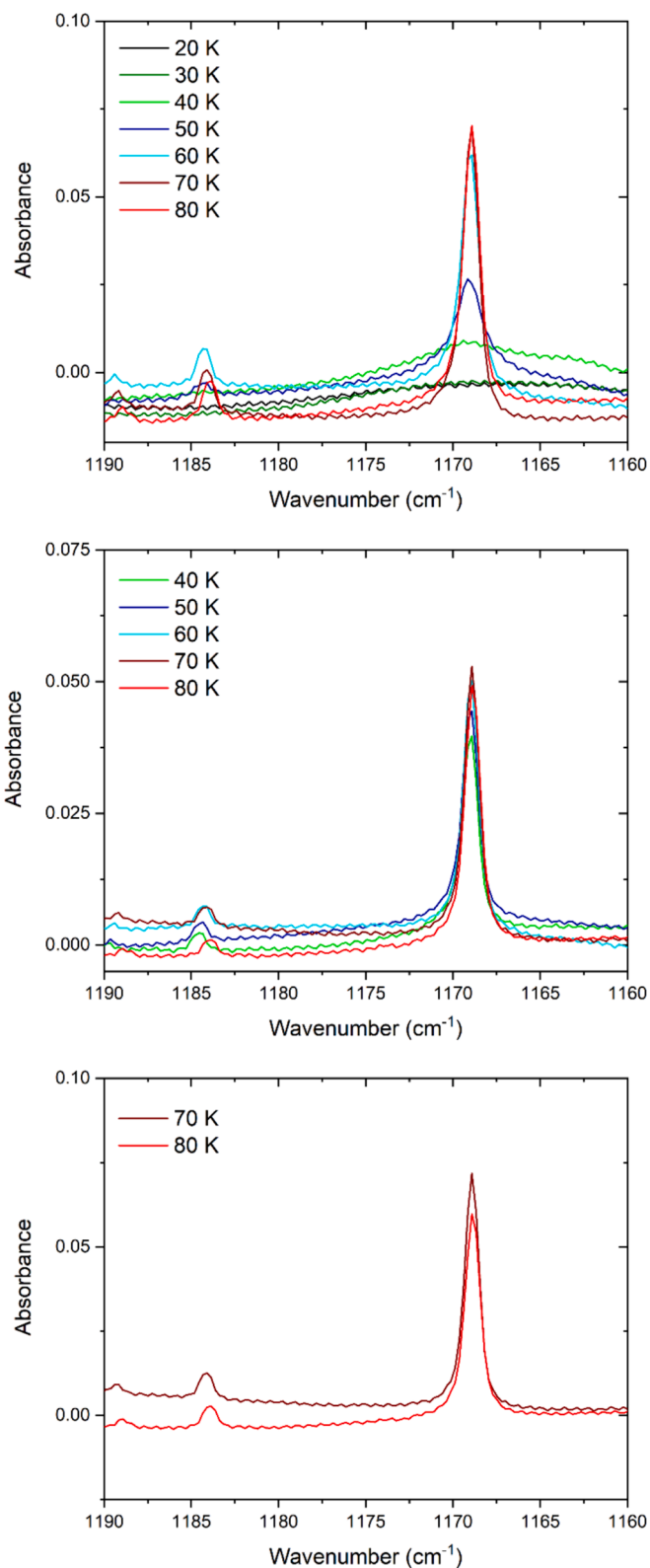
Fig. 4. Thermal evolution of the band attributed to the H_2S ν_2 modes for ices deposited at 20, 40, and 70 K. Note the readily observable presence of the individual ν_2 (E_u), and ν_2 (A_{2u}) modes (in order from highest to lowest wavenumber position) in the crystalline ices.

profile expected for a wholly crystalline ice, with bands for both the ν_2 (A_{2u}) and the ν_2 (E_u) modes (as well as bands for the ν_3, ν_1 (A_{2u}), and the ν_1 (E_u) modes) being immediately visible and undergoing very little variation in their appearance on warming to 80 K.

As with the ν_s modes, we have performed an analysis of the variation in the band peak position of the ν_2 mode as a function of temperature for the three ices considered in this study. As can be seen in Fig. 5, there was very little variation in peak position of the ν_2 (A_{2u}) band, irrespective of the deposition temperature of the H_2S ice. Indeed, the maximum shift in the wavenumber position of this band was found to be 0.3 cm^{-1}, which is similar to the $\pm$ 0.25 cm^{-1} uncertainty associated with our measurements of this parameter. The less intense ν_2 (E_u) band was, however, noted to undergo a red-shift in its position as a result of the thermal processing of the H_2S ice. In the case of the ices deposited at 20, 40, and 70 K, the maximum red-shift experienced upon warming to 80 K was found to be 0.5, 0.7, and 0.2 cm^{-1}, respectively.

An analysis of the variation in the peak height (in this case, defined as the maximum absorbance of the ν_2 (A_{2u}) band) relative to its value upon the first appearance of the band) has also been performed (Fig. 5). In the case of the H_2S ice deposited at 20 K, a band corresponding to the ν_2 mode first appeared at a temperature of 40 K, and thus its height at this temperature was taken to be the initial value H_0. Thermal processing of the ice deposited at 20 K to 70 K resulted in the peak height more than quadrupling its initial value, before declining slightly on annealing to 80 K as a result of some sublimation-induced losses. A qualitatively similar, yet quantitatively more modest, trend was noted for the ice deposited at 40 K, for which the band peak height of the ν_2 mode increased by just shy of 40 % of its initial value on warming to 70 K, before decreasing again on transitioning to 80 K. In the case of the H_2S ice deposited at 70 K, a modest decrease in the band peak height was noted upon warming to 80 K, again due to sublimation-induced losses of the ice. It should be noted that, unfortunately, the uncertainties associated with the measurement of the integrated absorbance of the bands associated with the ν_2 mode are too large for an accurate analysis to be performed, due primarily to the weak intensities of these bands. As such, no analysis of the effect of thermal processing on the integrated absorbance of these bands has been carried out.

3.3. Comparisons with previous studies

The infrared absorption spectroscopy of solid H_2S has been a subject of interest for close to seven decades, with a number of studies having reported on the major absorption features of this molecule and its isotopologues [22–29]. However, as was previously stated, arguably the most detailed study (prior to the systematic experiments described herein) was that of Fathe et al. [27], which reported the spectra of amorphous and crystalline H_2S and D_2S ices respectively prepared by deposition of the gases at 10 and 70 K. There are a number of similarities

between our experiments and those of Fathe et al. [27]; for instance, both studies made use of a cryogenically cooled ZnSe surface as the deposition substrate on which H_2S ices were prepared, and the overall thicknesses of the amorphous (circa 0.8–0.9 µm) and crystalline (0.4–0.5 µm) ices prepared in both studies were very similar.

However, there are also a number of differences between our work and that of Fathe et al. [27], both in terms of the experimental apparatus and methodology used, as well as the results obtained. Starting with the former, we note that the ICA set-up operates at a significantly lower base pressure (10^{-9} mbar) than the experimental set-up used by Fathe et al. [27] (10^{-6} mbar). The lower base pressure at the ICA means that there is a reduced likelihood of contamination of our H_2S ices by so-called background molecules such as H_2O, N_2, or O_2. Although there is nothing in the results of Fathe et al. [27] that would suggest that their ices suffered from any such contamination, it is nonetheless desirable to access lower chamber base pressures so as to not only minimise any such contamination, but to also better replicate the ultrahigh-vacuum conditions found in many astronomical settings.

Methodological differences also exist between the present study and that of Fathe et al. [27], most notably in the fact that that study only considered the spectra of ices deposited and held at two fixed temperatures (i.e., 10 and 70 K), whereas the effect of thermal processing on the spectra was systematically examined in our study for H_2S ices deposited at three different temperatures (i.e., 20, 40, and 70 K). Moreover, although the study of Fathe et al. [27] acquired spectra over a wider wavenumber range (6000–500 cm^{-1} compared to our 4000–650 cm^{-1}), these spectra were acquired at a lower resolution (2 cm^{-1} compared to our 0.5 cm^{-1}) and using fewer co-added scans (100 compared to our 256).

Despite these differences, it is to be noted that there is generally very good agreement between our spectroscopic results and those of Fathe et al. [27], at least in terms of the infrared band profiles and positions of the fundamental absorption modes of the amorphous and crystalline H_2S ices; indeed, the reported wavenumber positions of the bands attributable to the ν_1 (E_u), ν_1 (A_{2u}), ν_2 (E_u), ν_2 (A_{2u}), and ν_3 modes all match within 3 cm^{-1}, with most matching within 1 cm^{-1} (Table 1). It is to be noted, however, that there are greater discrepancies between the wavenumber positions of absorption bands associated with the higher wavenumber combination modes of solid H_2S as reported by Fathe et al. [27] and this present study (Table 1).

For instance, the $\nu_1 + \nu_2$ combination mode in a 70 K crystalline ice is located at 3682 cm^{-1} in the study of Fathe et al. [27] (which matches well with the 3683 cm^{-1} position reported by Ferraro et al. [26] for a crystalline ice at 89 K), but is notably blue-shifted to 3694.3 cm^{-1} in our study (Table 1). The origin of this discrepancy is not known for certain; however, it is to be recalled that the combination bands in the infrared absorption spectrum of solid H_2S are very weak features, and thus their measurement may be associated with higher uncertainties. It is therefore
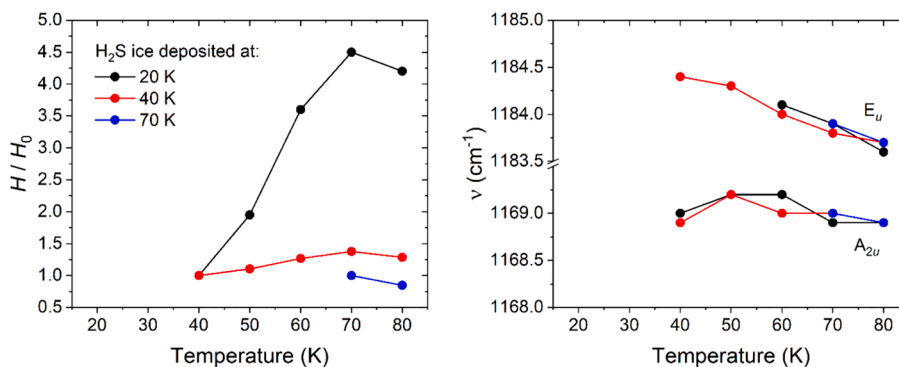
Fig. 5. Variations in peak height H (left panel) and peak positions ν (right panel) of the ν_2 modes for H_2S ices deposited at 20 (black circles), 40 (red circles), and 70 K (blue circles). Note that the variations in H are reported relative to their initial values H_0 upon deposition of the ice. Error bars have been omitted for clarity, but upper bounds to the uncertainties associated with H / H_0, and ν have been calculated to be $\pm$ 15 %, and $\pm$ 0.25 cm^{-1}, respectively.

recommended that future studies dedicated to better spectroscopically characterising the combination modes of solid H_2S be performed. Nevertheless, it is the fundamental absorption modes that are most likely to be of use to the astrochemistry research community in the detection of solid H_2S in astronomical environments and there is very good agreement in the reported positions and profiles of the bands associated with these absorption modes between our present study and previous works, as described previously. Our quantitative analyses of the thermally induced changes to these absorption bands (Figs. 2-5) therefore represent an important step forward in our understanding of the infrared absorption spectroscopy of solid H_2S under conditions relevant to astrochemistry.

4. Conclusions

In this paper, we have provided a discussion of the results of a thorough and systematic mid-infrared spectroscopic analysis of the absorption bands associated with the stretching (ν_s) and bending (ν_2) modes of H_2S ices deposited at different temperatures and thermally processed under conditions relevant to astrochemistry. Our results have demonstrated that, when deposited at 20 K, H_2S ice is amorphous in structure and its crystallisation may be thermally induced by warming in a process that is largely complete by 60 K. This thermally induced phase change was evidenced in acquired mid-infrared absorption spectra through the resolution of the broad band attributed to the ν_s mode into its constituent ν_3, ν_1 (E_u), and ν_1 (A_{2u}) sub-components. This change in the appearance of the absorption spectrum was accompanied by the appearance of a band attributable to the ν_2 mode, which was not visible at 20 K. By 60 K, however, this band not only adopted the narrow profile anticipated for crystalline ices, but also underwent splitting into its individual ν_2 (E_u) and ν_2 (A_{2u}) bands.

Our results have also provided evidence for the fact that the temperature at which an ice is prepared under conditions relevant to astrochemistry plays a key role in the resultant degree of crystallinity of that ice. In particular, we have demonstrated that H_2S ices deposited at 40 K will be characterised by significantly more ordered structures than an analogous ice deposited at 20 K and subsequently warmed to 40 K. Such a result is broadly in agreement with a growing body of literature that suggests that amorphous ices deposited at higher temperatures undergo more extensive structural reorganisation to crystalline phases when subjected to thermal processing. It is to be noted that, in our experiments, the H_2S ice deposited at 70 K exhibited spectroscopic features characteristic of a wholly crystalline ice throughout its thermal processing.

The results described in this paper are directly relevant to aiding the as yet unsuccessful detection of H_2S ice in interstellar and circumstellar environments, as they provide a laboratory-generated benchmark against which observational data collected by high-resolution and high-sensitivity instruments such as the *James Webb Space Telescope* may be compared. Furthermore, forthcoming missions to the outer Solar System, such as the *Jupiter Icy Moons Explorer* and the *Europa Clipper* missions to the Jovian moon system, will be equipped with infrared imaging spectrometers which will not only allow for novel detections of H_2S ices on the surfaces of these moons, but may also allow for their distributions to be accurately mapped. Such detections and mappings would provide an insight into the sulphur cycles of these icy moons, and thus allow for a further constraining of their astrobiological potential to host extraterrestrial life.

CRediT authorship contribution statement

Duncan V. Mifsud: Conceptualization, Methodology, Formal analysis, Investigation, Writing – original draft, Writing – review & editing. **Péter Herczku:** Methodology, Investigation. **Ragav Ramachandran:** Methodology, Investigation. **Pavithraa Sundararajan:** Methodology, Investigation. **K.K. Rahul:** Methodology, Investigation. **Sándor T.S.**
Kovács: Methodology, Investigation. **Béla Sulik:** Validation, Supervision. **Zoltán Juhász:** Validation, Supervision. **Richárd Rácz:** Methodology, Investigation. **Sándor Biri:** Methodology, Investigation. **Zuzana Kaňuchová:** Formal analysis, Data curation. **Sergio Ioppolo:** Supervision, Resources. **Bhalamurugan Sivaraman:** Supervision. **Robert W. McCullough:** Supervision. **Nigel J. Mason:** Supervision, Resources, Project administration, Funding acquisition.

Declaration of competing interest

The authors declare that they have no known competing financial interests or personal relationships that could have appeared to influence the work reported in this paper.

Data availability

Data will be made available on request.

Acknowledgements

References

[1] B.A. McGuire, Astrophys. J. Suppl. Ser. 259 (2022) 30.
[2] R.C. Fortenberry, Int. J. Quantum Chem 117 (2017) 81–91.
[3] C. Puzzarini, V. Barone, PCCP 22 (2020) 6507–6523.
[4] A.C.A. Boogert, P.A. Gerakines, D.C.B. Whittet, Ann. Rev. Astron. Astrophys. 53 (2015) 541–581.
[5] A.L. Mattioda, D.M. Hudgins, C. Boersma, et al., Astrophys. J. Suppl. Ser. 251 (2020) 22.
[6] W.R.M. Rocha, M.G. Rachid, B. Olsthoorn, et al., A & A 668 (2022) A63.
[7] D.V. Mifsud, Z. Kaňuchová, S. Ioppolo, et al., J. Mol. Spectrosc. 385 (2022) 111599.
[8] D.V. Mifsud, Z. Kaňuchová, S. Ioppolo, et al., PCCP 24 (2022) 18169–18178.
[9] D.V. Mifsud, P. Herczku, K.K. Rahul, et al., PCCP 25 (2023) 26278–26288.
[10] D.V. Mifsud, Z. Kaňuchová, P. Herczku, et al., Space Sci. Rev. 217 (2021) 14.
[11] M.K. McClure, W.R.M. Rocha, K.M. Pontoppidan, et al., Nat. Astron 7 (2023) 431–443.
[12] S.D. Rodgers, S.B. Charnley, Adv. Space Res. 38 (2006) 1928–1931.
[13] U. Calmonte, K. Altwegg, H. Balsiger, et al., MNRAS 462 (2016) S253–S273.
[14] M. Rubin, K. Altwegg, H. Balsiger, et al., MNRAS 489 (2019) 594–607.
[15] H. Linnartz, S. Ioppolo, G. Fedoseev, Int. Rev. Phys. Chem. 34 (2015) 205–237.
[16] S. Ioppolo, H.M. Cuppen, C. Romanzin, et al., Astrophys J 686 (2008) 1474–1479.
[17] D. Qasim, G. Fedoseev, K.J. Chuang, et al., Nat. Astron 4 (2020) 781–785.

[18] G. Fedoseev, S. Ioppolo, D. Zhao, et al., MNRAS 446 (2015) 439–448.
[19] N. Watanabe, A. Kouchi, Astrophys J 571 (2002) L173.
[20] A. Michaelides, P. Hu, J. Chem. Phys. 115 (2001) 8570–8574.
[21] Y. Liu, W. Guo, X. Lu, et al., RSC Adv. 6 (2016) 6289–6299.
[22] F.R. Reding, D.F. Hornig, J. Chem. Phys. 27 (1957) 1024–1030.
[23] R.W. Miller, G.E. Leroi, J. Chem. Phys. 49 (1968) 2789–2797.
[24] A. Anderson, O.S. Binbrek, H.C. Tang, J. Raman Spectrosc. 6 (1977) 213–220.
[25] J.R. Ferraro, U. Fink, J. Chem. Phys. 67 (1977) 409–413.
[26] J.R. Ferraro, G. Sill, U. Fink, Appl. Spectrosc. 5 (1980) 525–533.
[27] K. Fathe, J.S. Holt, S.P. Oxley, et al., J. Phys. Chem. A 110 (2006) 10793–10798.
[28] R.L. Hudson, P.A. Gerakines, Astrophys J 867 (2018) 138.
[29] Y.Y. Yarnall, R.L. Hudson, The Astrophysical Journal Letters 931 (2022) L4.
[30] J.K. Cockroft, A.N. Fitch, Z. Krist. 193 (1990) 1–19.
[31] A.N. Fitch, J.K. Cockroft, J. Chem. Soc. Chem. Commun. (1990) 515–516.
[32] W.Y. Zeng, A. Anderson, J. Raman Spectrosc. 32 (2001) 9–15.
[33] P. Herczku, D.V. Mifsud, S. Ioppolo, et al., Rev. Sci. Instrum. 92 (2021) 084501.
[34] D.V. Mifsud, Z. Juhász, P. Herczku, et al., Eur. Phys. J. D 75 (2021) 182.
[35] Y.Y. Yarnall, R.L. Hudson, Icarus 373 (2022) 114799.
[36] R. Luna, G. Molpeceres, J. Ortigoso, et al., A & A 617 (2018) 116.
[37] R. Luna, C. Millán, M. Domingo, et al., Astrophys J 935 (2022) 134.
[38] P.A. Gerakines, R.L. Hudson, Astrophys. J. Lett. 805 (2015) L20.
[39] P.A. Gerakines, R.L. Hudson, Astrophys. J. Lett. 808 (2018) L40.
[40] R.L. Hudson, M.J. Loeffler, P.A. Gerakines, J. Chem. Phys. 146 (2017) 024304.